Behavior Analysis of Galfenol Beam Vibration Energy Harvester

著者（英）	Rezaeealam Behrooz, Ueno Toshiyuki, Yamada Sotoshi
journal or publication title	Journal of the Japan Society of Applied Electromagnetics and Mechanics = 日本AEM学会誌
volume	20
number	1
page range	138-143
year	2012
ISSN	0919-4452
URL	http://doi.org/10.24517/00048915

学術論文

Behavior Analysis of Galfenol Beam Vibration Energy Harvester

Behrooz REZAEEALAM[*1] (Mem.), Toshiyuki UENO[*1] (Mem.) and Sotoshi YAMADA[*1] (Mem.)

This paper describes a static finite element model of magnetostrictive materials, considering magnetic and elastic boundary value problems that are bidirectionally coupled through stress and field dependent variables. The finite element method is applied to a small vibration-driven generator of magnetostrictive type employing Iron-Gallium alloy (Galfenol) for the purpose of the behaviour analysis of the Galfenol beams under bending conditions by illustrating the spatial variations in stress and magnetic field and finally the numerical results are compared with the experimental ones.

Keywords: magnetostrictive material, vibration energy harvester, finite element method.

1. Introduction

The development of new magnetostrictive alloys has improved the possibilities to build devices based on magnetostrictive phenomenon. Contrary to Terfenol-D, Galfenol's high strength and ductility have made it a popular option for research in sensing and actuator applications involving bending [1].

Experimental studies on sensors and actuators involving bending mode [2, 3] have been performed using Galfenol unimorph sensors and laminated composites having Galfenol attached to other structural materials. The vibrating device inspected in this paper, which is functionally similar to cantilevers, consists of two Galfenol beams that reciprocally one beam is compressed and the other one is stretched [4, 5].

In order to investigate the behavior of Galfenol in bending conditions, a model for simulation of the vibration energy harvester, based on static finite element method and static measurements, has been developed. The bending-induced stress leads not only to a non-uniform distribution of permeability but also to a non-uniform distribution of magnetostriction for an applied magnetic field. Conversely, the magnetostriction alters the stress distribution in the Galfenol beam; therefore it is necessary to consider the bidirectional coupling between magnetic and mechanical problems. Contrary to the models previously developed and based on a strong coupling approach of magnetostrictive problem [6], the approach employed in this paper is based on a so-called weak coupling approach [7].

The multiphysics finite element package FEMLAB [7] allows the magnetostrictive strain tensor to be implemented directly using the actual properties of the materials involved within the system. Finally, experimental results are presented which show the agreement between the numerical derivations and experimental results.

Correspondence: B. REZAEEALAM, Institute of Nature and Environmental Technology, Kanazawa University, Kakuma, Kanazawa 920-1192, Japan
email: behrooz@magstar.ec.t.kanazawa-u.ac.jp
[*1] Kanazawa University

2. Configuration of the Vibration Energy Harvester

The energy harvester consists of two parallel square rod of Galfenol ($Fe_{81.6}Ga_{18.4}$, 0.5mm by 1mm area and 10mm length, magnetically easy axis in longitudinal direction) is shown in figures 1 and 2. On each Galfenol beam a coil of 312 turns is wound (0.05 mm diameter wire, 12 Ω). Before shaping to the beam, the Galfenol was stress-annealed under compressive stress to equip built-in uniaxial anisotropy such that flux variation is occurred under tensile as well as compressive stresses [1]. In addition, one yoke is bonded to a fixture and the other one to a mover (Al, 0.64g) which oscillates by external force. Two pieces of Nd-B-Fe permanent magnets (2mm diameter and 2mm length) are used to provide adequate bias flux for the beams and the attached back iron yokes close the magnetic circuit.

The fundamental operation principle of the energy harvester is based on the inverse magnetostrictive effect that the magnetization changes with the stress. When a bending load is applied to the mover, one Galfenol beam is compressed and the other one is stretched leading to relative permeability change in both Galfenol beams which causes the magnetic flux density to drop inside the compressed beam and to rise inside the stretched beam. Therefore, voltages are induced in the coils around Galfenol beams due to time-varying magnetic fields and the vibration energy is harvested.

3. Finite Element Modeling

3.1 Modeling of the Magnetic Aspect

In the magnetostatic case, a vector potential A formulation is quite sufficient to describe the magnetic problem and it is formulated by the following equations:

$$J = \nabla \times \left(\frac{1}{\mu_0 \mu_r(\sigma, H)} \nabla \times A \right) \quad (1)$$

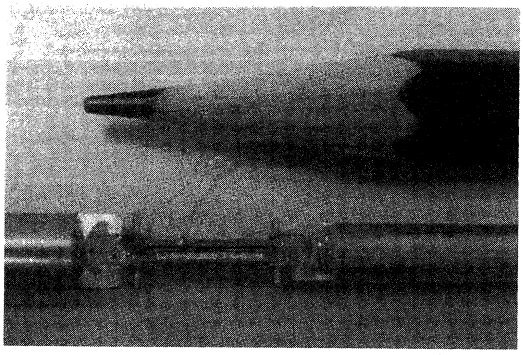

Fig. 1. The fabricated device.

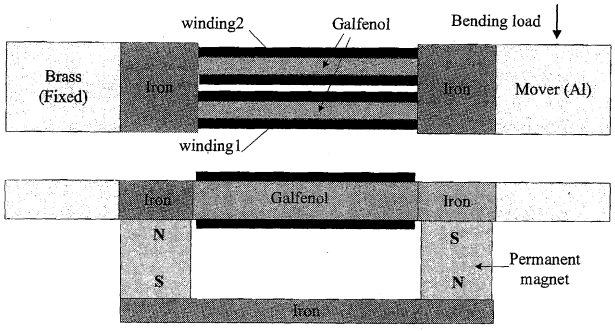

Fig. 2. Sectional view of the device.

$$\mu_r(\sigma,H)=\frac{\nabla\times\boldsymbol{A}}{\mu_0 H} \tag{2}$$

$$\mu_r(\sigma,H)=\frac{\boldsymbol{B}}{\mu_0 H} \tag{3}$$

where B is the flux density, H is the flux intensity, σ is the mechanical stress and $\mu_r(\sigma,H)$ is the relative permeability which varies depending on mechanical stress and magnetic field in the Galfenol beams.

3.2 *Modeling of the Mechanical Aspect*

In the static case, the mechanical problem is formulated by the following equations:

$$\nabla\cdot\sigma+F_{body}=0 \tag{4}$$

$$\varepsilon=\nabla u \tag{5}$$

$$\sigma_x=E\frac{(1-\upsilon)(\varepsilon_x-\lambda(\sigma,H))+\upsilon\varepsilon_y+\upsilon\varepsilon_z}{(1+\upsilon)(1-2\upsilon)} \tag{6}$$

$$\sigma_y=E\frac{\upsilon(\varepsilon_x-\lambda(\sigma,H))+(1-\upsilon)\varepsilon_y+\upsilon\varepsilon_z}{(1+\upsilon)(1-2\upsilon)} \tag{7}$$

$$\sigma_z=E\frac{\upsilon(\varepsilon_x-\lambda(\sigma,H))+\upsilon\varepsilon_y+(1-\upsilon)\varepsilon_z}{(1+\upsilon)(1-2\upsilon)} \tag{8}$$

where F_{body} is the body force, E is the Young's modulus, υ the poisson coefficient, u the displacement, ε the mechanical strain and λ(σ,H) is the magnetostriction's contribution to strain, which varies depending on mechanical stress and flux density in the Galfenol beams. When calculating the stress, it is necessary to subtract the contribution of magnetostriction from the corresponding strain in the direction of elongation ([001] direction) [2].

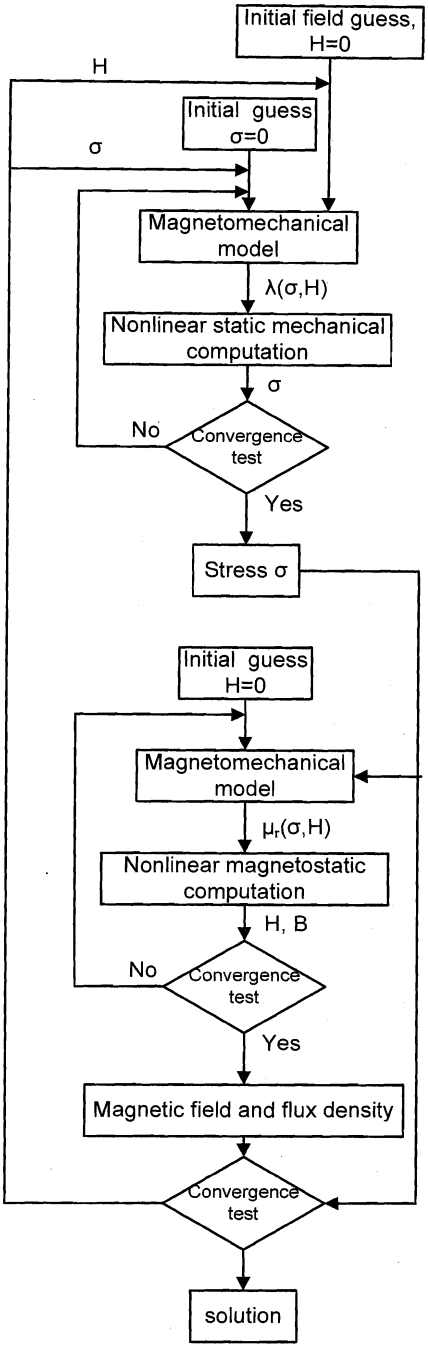

Fig. 3. Diagram of the weak coupling approach.

3.3 *Weak Coupling Approach*

The coupled problem is treated by an iterative process of successive magnetic and mechanical finite element computations [7]. Figure 3 illustrates the diagram of the weak coupling approach that has been implement by COMSOL Multiphysics software. It

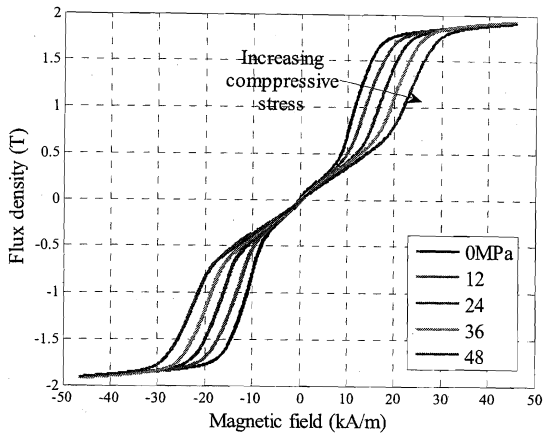

(a) B(σ,H) curves

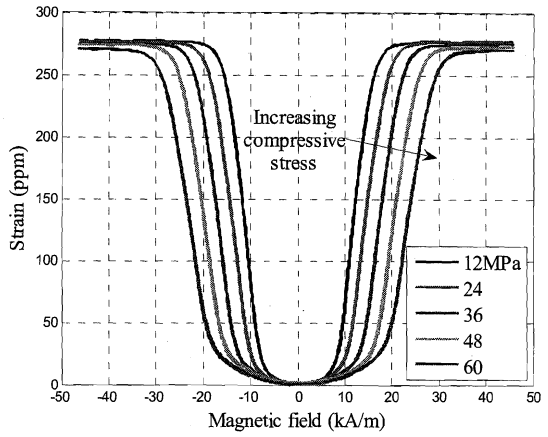

(b) λ(σ,H) curves

Fig. 4. Experimental magnetization and magnetostriction curves in the direction of [001].

includes two segregated steps, one step for magnetostatic problem while the mechanical variables are considered constant, and another step for mechanical problem in which the magnetic variables are considered constant.

The highly nonlinear behavior of Galfenol is modeled well by fitting the Armstrong energy-based model to experimental λ-H and B-H characterization curves. Figure 4 shows the experimentally determined magnetization curves B(σ,H) and magnetostriction curves λ(σ,H) for a $Fe_{81.6}Ga_{18.4}$ sample. The magnetostriction λ(σ,H) is defined as the initial strain for mechanical boundary value problems in order to subtract the contribution of magnetostriction from the corresponding strain in the direction of elongation that has been expressed in equations (6-8). It is worth noting that the mechanical problem is solved by an iterative scheme due to the dependence of λ(σ,H) on the applied stress σ.

4. Results

The applied magnetic field is created by two pieces of permanent magnet with a remanent flux density of 0.7 T and the spatial distribution of magnetic field is

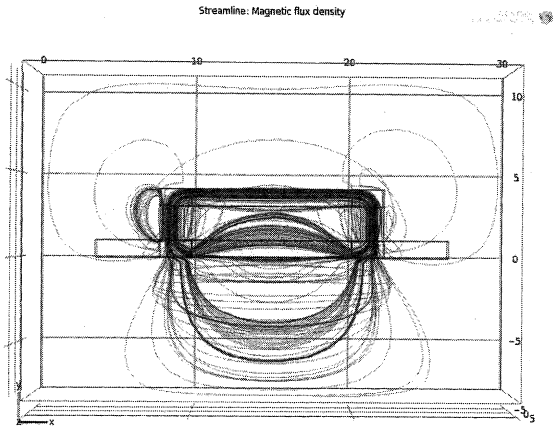

Fig. 5. Spatial distribution of magnetic field in x-y view.

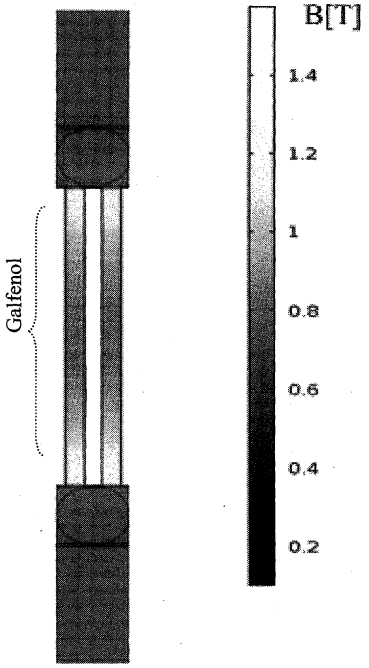

Fig. 6. Magnetic flux density B_x distribution in a cut view through Galfenol beams without bending load.

shown in figure 5, also figure 6 displays the magneti flux density in a slice cut through the Galfenol beams. I is clear that the magnetic flux scatters around the Galfe nol beam owing to the lower permeability of Galfenc compared with that of back-iron. It can also be seen tha magnetic saturation occurs at both ends of the Galfenc beams, however the size of the permanent magnets ha been chosen in the way that the average x-component c flux density ([001] direction) inside the Galfenol beam is 0.83 T as the bias magnetic field without bending loa The average x-component of magnetic flux density calculated as:

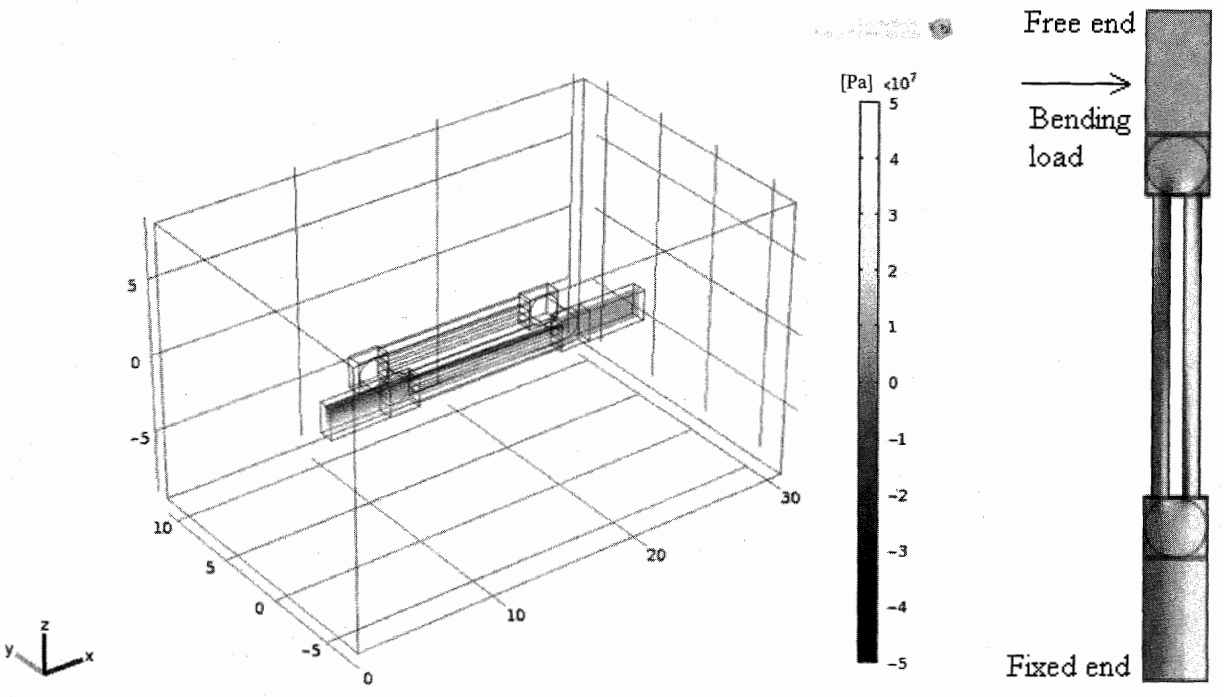

Fig. 7. Spatial distribution of stress σ_x in the beams.

$$B_{x\text{-ave}} = \frac{1}{V}\iiint B_x dv \tag{9}$$

where V is the volume of the Galfenol beam. Figure 7 depicts the vibration energy harvester in 3D and shows a slice cut through the Galfenol beams that demonstrates the stress distribution inside it, caused by 2 N bending force perpendicular to the free end. As a matter of fact the bending device is similar to a cantilever as one of the beams is compressed while the other one is stretched.

Figure 8 shows the corresponding alterations to spatial distribution of relative permeability inside the Galfenol beams caused by compressive and tensile stresses. The relative permeability of the compressed beam tends to decrease and the relative permeability of the stretched beam tends to increase. It can be seen that the relative permeability of Galfenol ranges between 30 and 180 and it's worth mentioning that relative permeability is obtained by equation (3).

Furthermore, figure 9 demonstrates the corresponding variations in spatial distribution of the x-component of the magnetic flux density inside the Galfenol beams as the flux density decreases in the compressed beam and increases in the stretched beam.

The average flux densities $B_{x\text{-ave}}$ as a function of applied bending force are presented in figure 10. The average flux density in the stretched beam increases from the bias point of 0.83 T to 1.45 T, while it decreases from the bias point of 0.83T to 0.6T in the compressed beam. The average flux densities do not almost vary by applying forces larger than 4 N due to magnetic and magnetostrictive saturation.

Figures 11 and 12 show the mean of flux densities in three cross-sections of the beams which are calculated as:

$$B_{x\text{-ave-s}} = \frac{1}{S}\iint B_x ds \tag{10}$$

where S is the area of the cross-section, and they are drawn versus the applied bending force. Figure 11 depicts the flux density differential between the two beams in the middle of them and figure 12 also depicts the flux density differential at the cross-sections 2 and 4. They demonstrate that the change in flux density in the middle of the beams is higher than the other parts, and in addition, at the cross-section 4 which is closer to the free end of the energy harvester, the flux density differential between the two beams becomes higher than the one at cross-section 2 owing to the related spatial stress distribution inside the Galfenol beams.

Experimental implementation was carried out by vibrating the device at the resonance frequency of 333 Hz, hence the bending stress leads to changes in magnetic flux density in both the compressed and stretched beams and results in the time-varying magnetic flux density. The displacement of the free end of the device was measured by laser sensor, and also pick-up sensing coils were used to measure the magnetic flux density at the desired cross-sections of the Galfenol beams. It is noteworthy that the pick-up coils measure the differen-

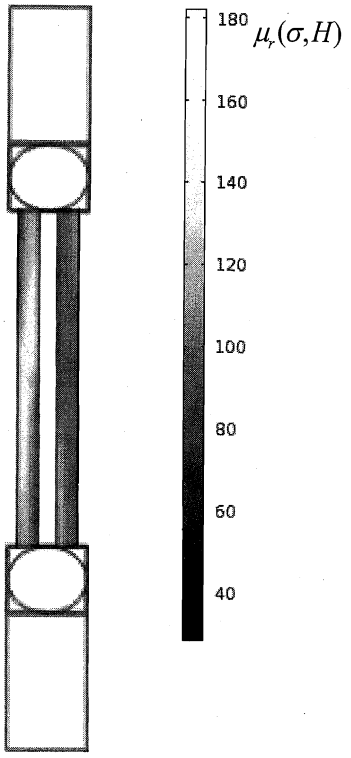

Fig. 8. Spatial distribution of relative permeability in the Galfenol beams.

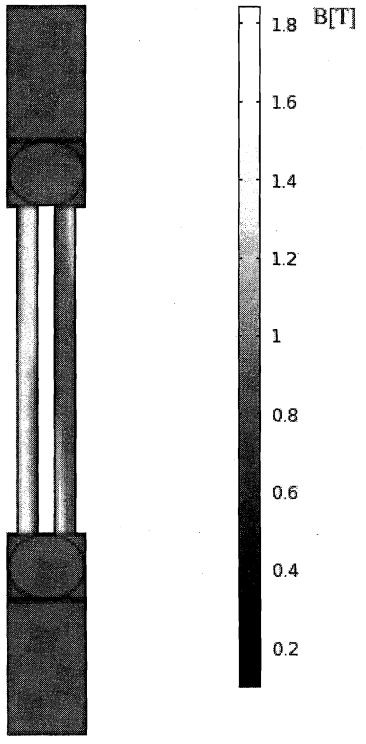

Fig. 9. Spatial distribution of magnetic flux density B_x in the Galfenol beams.

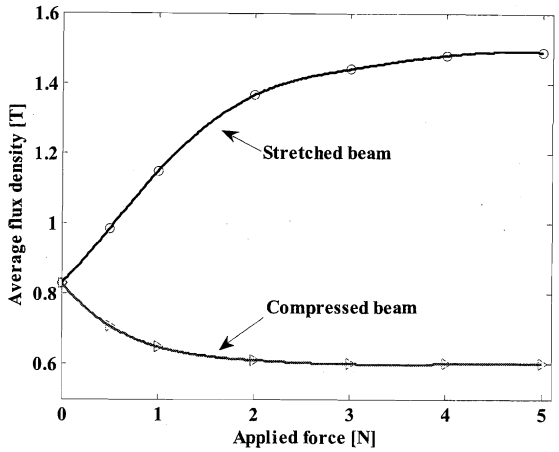

Fig. 10. Average flux density $B_{x\text{-}ave}$ inside the two Galfenol beams.

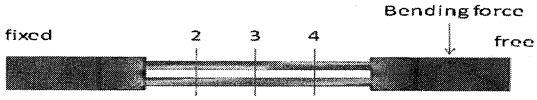

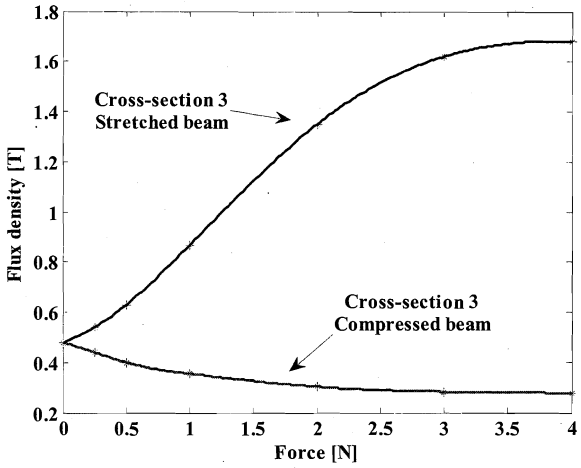

Fig. 11. Flux density differential between the two beams at cross-section 3.

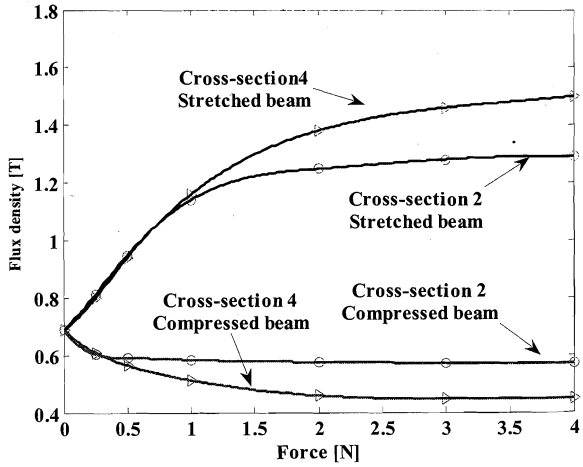

Fig. 12. Flux density differential between the two beams at cross-sections 2 and 4.

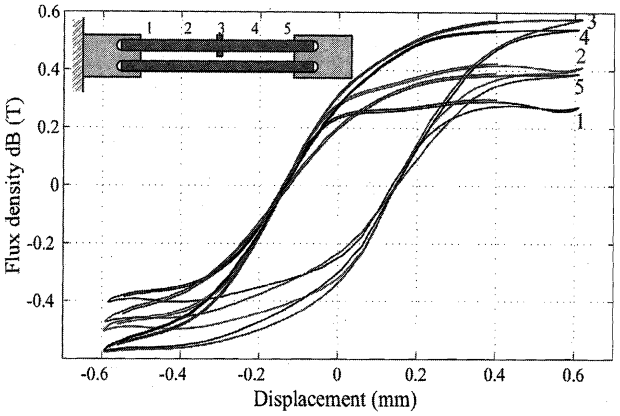

Fig. 13. Measured differential flux density between two Galfenol beams at five cross-sections versus the displacement of the free end.

tial of the magnetic flux density between the two parallel beams.

Figure 13 shows the resultant flux density versus the displacement caused by beam deflection [5]. The presence of hysteresis in curves is mainly due to the back-iron of the device while the Galfenol beams present negligible hysteresis. It can be seen that the maximum variation in the magnetic flux density occurs in the middle of the Galfenol beams and about 1.2 T change in magnetic flux density is achieved which agrees with the predicted value by the 3-D static finite element analysis. The simulation results are quite coherent with the magnetostriction phenomenon, although the experimental results differ from those obtained from the numerical method at the cross-sections 2 and 4, because the employed static finite element method does not consider eddy currents and hysteresis, and also the exact mechanical properties of the back-iron, permanent magnets and Galfenol beam such as Young's modulus are unknown.

5. Conclusion

The 3-D static finite element modeling presented here highlights the spatial variations in magnetic field and relative permeability due to the corresponding stress distribution in the Galfenol beams subjected to bending load. The maximum variation in the magnetic flux density occurs in the middle of the Galfenol beams and about 1.2 T change in magnetic flux density is achieved which demonstrates the effectiveness of the inspected vibration-driven generator in voltage generation and energy harvesting. The model predictions agree with the experimental results and are coherent with the magnetostriction phenomenon.

(Received: 30 March 2011/Revised: 9 September 2011)

References

[1] M. Wun-Fogle, J. B. Restorff and A. E. Clark, "Magnetomechanical Coupling in Stress-Annealed Fe-Ga (Galfenol) Alloys," *IEEE Trans. Magnetics*, Vol. 42, pp. 3120-3122, 2006.

[2] C. Mudivarthi, S. Datta, J. Atulasimha and A. B. Flatau, "A Bidirectionally Coupled Magnetoelastic Model and its Validation using a Galfenol Unimorph Sensor," *Smart Materials and Structures*, Vol.17, pp.1-8, 2008.

[3] S. Datta, "Quasi-Static Characterization and Modelling of the Bending Behaviour of Single Crystal Galfenol for Magnetostrictive Sensors and Actuators," *Dissertation*, Maryland University, 2009.

[4] T. Ueno, S. Yamada and Y. Ikehata, "Micro Magnetostrictive Energy Harvester using Iron Gallium Alloy (Galfenol)," *in Proceedings of 55th Magnetism and Magnetic Materials Conference,* Atlanta, 2010.

[5] T. Ueno and S. Yamada, "Study on Micro-energy Harvesting Device Using Iron-Gallium Alloy", *J. Magn. Soc. Jpn.*, Vol. 35, pp. 88-91, 2011.

[6] P. G. Evans and M. J. Dapino, "Dynamic Model for 3-D Magnetostrictive Transducers," *IEEE Trans. Magnetics*, Vol. 47, pp. 221-230, 2010.

[7] COMSOL, MULTIPHYSICS © (FEMLAB), [online]. http://www.comsol.com